First Light of SINFONI at the VLT

SINFONI is an Adaptive Optics assisted cryogenic Near Infrared Spectrograph developed by ESO and MPE in collaboration with NOVA. It was successfully commissioned between June and August at the Cassegrain focus of VLT UT4 (Yepun). The instrument will be offered to the community from April 2005 onwards (period 75) and will provide a unique facility in the field of high spatial and spectral resolution studies of compact objects (star-forming regions, nuclei of galaxies, cosmologically distant galaxies, galactic centre etc.).

Henri Bonnet[1], Roberto Abuter[2], Andrew Baker[2], Walter Bornemann[2], Anthony Brown[8], Roberto Castillo[1], Ralf Conzelmann[1], Romuald Damster[1], Richard Davies[2], Bernard Delabre[1], Rob Donaldson[1], Christophe Dumas[1], Frank Eisenhauer[2], Eddie Elswijk[9], Enrico Fedrigo[1], Gert Finger[1], Hans Gemperlein[2], Reinhard Genzel[2,3], Andrea Gilbert[2], Gordon Gillet[1], Armin Goldbrunner[2], Matthew Horrobin[2], Rik ter Horst[9], Stefan Huber[2], Norbert Hubin[1], Christof Iserlohe[2,4], Andreas Kaufer[1], Markus Kissler-Patig[1], Jan Kragt[9], Gabby Kroes[9], Matthew Lehnert[2], Werner Lieb[2], Jochen Liske[1], Jean-Louis Lizon[1], Dieter Lutz[2], Andrea Modigliani[1], Guy Monnet[1], Nicole Nesvadba[2], Jona Patig[1], Johan Pragt[9], Juha Reunanen[1], Claudia Röhrle[2], Silvio Rossi[1], Riccardo Schmutzer[1], Ton Schoenmaker[9], Jürgen Schreiber[2,5], Stefan Ströbele[1], Thomas Szeifert[1], Linda Tacconi[2], Matthias Tecza[2,6], Niranjan Thatte[2,6], Sebastien Tordo[1], Paul van der Werf[8], Harald Weisz[7]

[1]European Southern Observatory; [2]Max-Planck-Institut für Extraterrestrische Physik, Garching, Germany; [3]Department of Physics, UC Berkeley, USA; [4]Universität Köln, Germany; [5]Max-Planck-Institut für Astronomie, Heidelberg, Germany; [6]Oxford University, UK; [7]Ingenieurbüro Weisz, München, Germany; [8]Leiden Observatory, NOVA, The Netherlands; [9]Netherlands Foundation for Research in astronomy

The ESO STC recommended the construction of SINFONI ("Spectrograph for INtegral Field Observation in the Near-Infrared") in October 1997. The instrument was conceived as the combination of an Adaptive Optics facility (the AO-Module), developed by ESO, and SPIFFI (SPectrometer for Infrared Faint Field Imaging), a Near Infrared Integral Field Spectrograph developed by the MPE. It merges in one instrument the experience gained by ESO in Adaptive Optics (AO) with the development of the MACAO product line and the experience of MPE in integral field spectrometry with 3D, the world's first infrared integral field spectrometer.

A two year detailed design phase was initiated in 2000. At the final design review (2001), the board recommended the upgrade of the instrument to a higher spectral resolution (nearly 4000) with a 2048 by 2048 pixel infrared detector. NOVA joined the consortium at that time to undertake the development of the so-called '2K Camera' scaling the spectral images to the size of the new detector.

FUNCTIONALITIES

The AO correction is based on the analysis of the wavefront of a reference star picked up close to the science Field of View (FOV). The sharing of the Cassegrain FOV between the two sub-systems is realized by an infrared dichroic mounted at the entrance of the SPIFFI cryostat. The visible flux (450 to 1000 nm) is reflected towards the wavefront sensor and the infrared (1.05 to 2.45 µm) is transmitted to the science focal plane.

The AO reference star can be acquired up to one arcmin off-axis.

The optimum performance is achieved with stars brighter than $R = 12$ mag picked up within ~20 arcsec but fair correction can be obtained in good atmospheric conditions over the full 1×2 arcmin^2 FOV with stars up to $R = 17$ mag. The AO-Module also supports seeing-limited operations when no guide star is available.
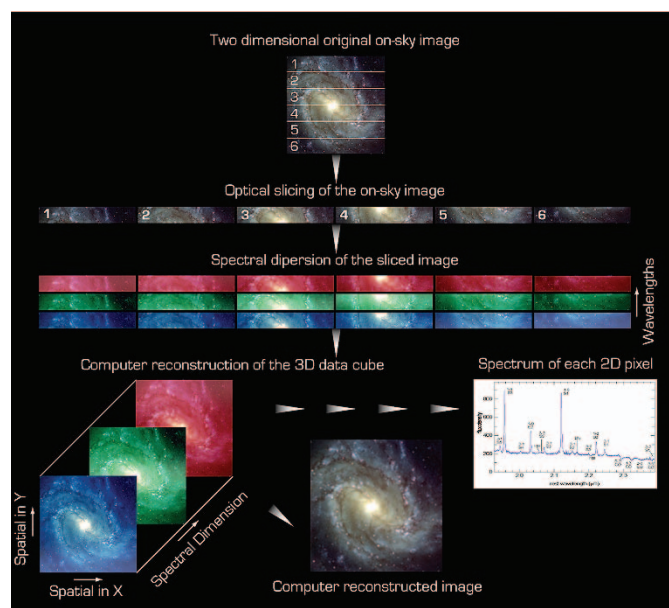

Figure 1: Principle of SPIFFI.

Figure 2: The AO-Module at the VLT UT4 Cassegrain focus for its stand-alone commissioning. The AO optical bench is the light-blue ring. It interfaces to the VLT Cassegrain flange through the AO-Housing (intermediate ring) and the interface flange (top dark ring). The yellow test structure simulates the mass of SPIFFI and provides the mechanical interface to the Infrared Test Camera (aluminum box in the yellow ring).
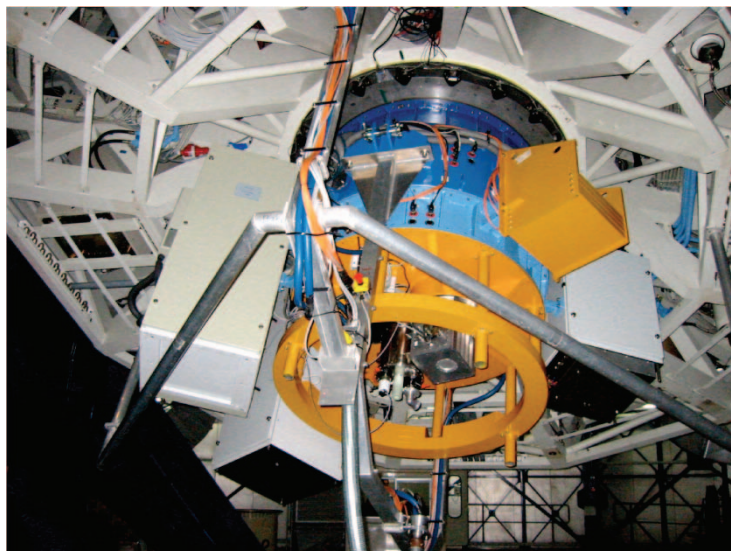
SPIFFI obtains spectra for each spatial element of its two-dimensional FOV. Its functional principle is shown in Fig. 1. After some processing of the raw data the outcome is a data cube, with 2 spatial (64 by 32 pixels) and one spectral (2048 pixels) dimensions. Spatially, three magnifications are offered. The high-resolution mode, with 25 mas$\times$ 12.5 (milli-arcsec) per pixel, provides a Nyquist sampling of the diffraction-limited Point Spread Function (PSF) at 2 μm with a narrow FOV (0.8×0.8 arcsec^2). This mode will offer spatially resolved spectral data on cosmologically distant galaxies, but will be limited by readout noise in many applications even in the case of long integrations (30 minutes). The intermediate pixel scale (100×50 mas/pixel) offers the best compromise between FOV, sensitivity and spatial resolution for most applications. The coarse mode (250×125 mas/pixel) is suitable for seeing-limited operations and also, thanks to its "wide" 8×8 arcsec^2 FOV, is very useful to help identifying the target during the acquisition.

Four spectroscopic modes are supported: the *J-, H-* and *K*-band gratings provide a spectral resolution of approx. 2000–4000. A lower resolution (~2000) is achieved with the combined *H* and *K* grating.

INSTALLATION AND COMMISSIONING SEQUENCE

The integration of SPIFFI with the "1K Camera" was completed at the beginning of 2002 in a configuration enabling a direct interface to the VLT for seeing-limited observations. SPIFFI was then operated as a guest instrument without AO for a period of three months, producing outstanding scientific data (see *The Messenger* 113, 17) as well as valuable experience in preparation for the AO-assisted operations. The instru-

ment was then shipped back to Europe and conditioned to interface to the AO-Module. The integration of the latter and its performance demonstration in the laboratory were completed in December 2003. The two subsystems were coupled for the first time in the ESO Garching integration facility in January 2004 and the Preliminary Acceptance in Europe was awarded in March. The 2K Camera and Detector assembly was then integrated in SPIFFI while the AO-Module was shipped to Chile for re-integration and stand-alone commissioning on the sky.

The first "AO" light was obtained on May 31st. On this occasion, an Infrared Test Camera was mounted at the AO-Module corrected focus to provide direct imaging capabilities (Fig. 2). The adaptive optics loop was immediately closed on a bright star ($m_V \sim 11$) and provided a corrected image concentrating into a diffraction-limited core 56% of the energy in the *K*-band ($\lambda = 2.2\mu$m, Figure 3). This performance conformed to expectations based on laboratory experi-

ments and the experience obtained with the two MACAO systems that had already been tested at the Coudé foci of the VLTs.

The re-integration of SPIFFI with the AO-Module took place in the assembly hall of Paranal in June and SINFONI first light was obtained on July 9 (Fig. 4). The first commissioning was devoted to the testing of all the observing modes and the tuning of the many automatic control loops which will ultimately make this complex instrument user-friendly. The success of the July run allowed for dividing the August commissioning run among commissioning activities for fine-tuning operations, Science Verification and Guaranteed Time Observations.

OPENING TO THE COMMUNITY

The instrument is currently equipped with an engineering-grade detector that is suitable for technical qualification but affected by flaws which would limit the science capabilities of SINFONI. The final science-grade detector is currently undergoing characterization tests in Garching and will be integrated in the instrument in November.

Meanwhile, the first call for proposals to the astronomical community will be issued in September and the start of regular observations is scheduled for Period 75 (starting April 1st 2005).

Adaptive Optics correction requires the presence of a reasonably bright reference star in the vicinity of the science target. This constraint limits AO operations to a small fraction of the sky. This limitation will be overcome as soon as Yepun (UT4) is equipped in 2005 with a Laser Guide Star Facility (LGSF). The LGSF will launch a 10W Sodium laser beam along the telescope line of sight to create an artificial beacon in the high atmospheric sodium layer (~100km), providing a reference for wavefront sensing. The upgrade of SINFONI to laser guide star operations is foreseen for the second quarter of 2005.

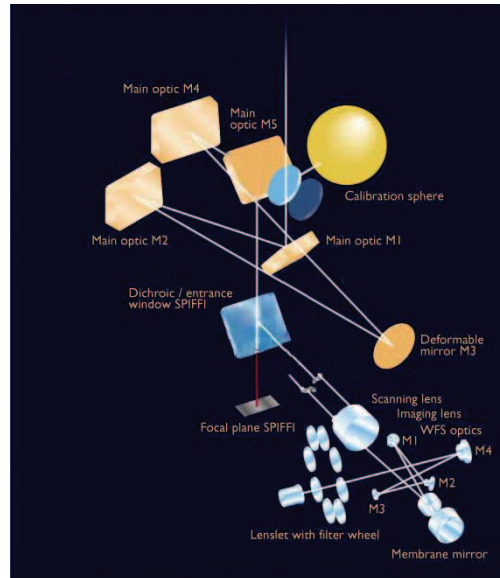**Figure 3:** AO-Module first light. The magnitude of the star is ~11 in *V*, the seeing 0.65 arcsec. The measured Strehl is 56% ($\lambda = 2.16$ μm). The displayed FOV is 0.5 arcsec, with a sampling of 15 mas/pixel.

60 Milli-arcseconds
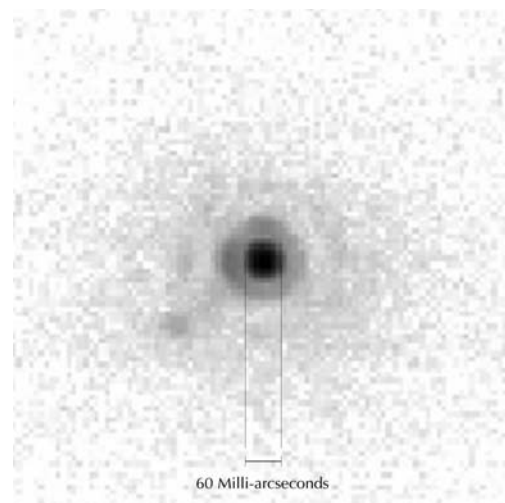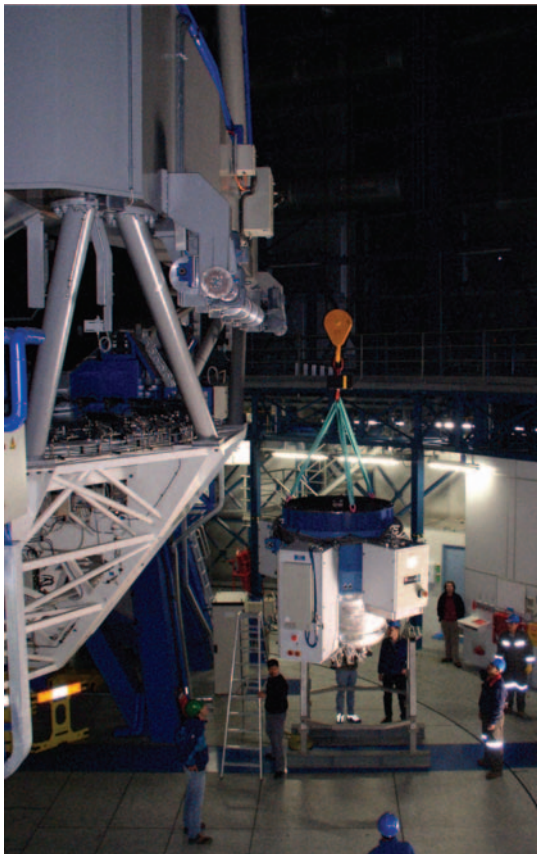
Figure 4: SINFONI during installation at UT4. The SPIFFI cryostat vessel is the grey aluminum part below the AO-Module (blue). To the left, the M1 cell of the VLT.

Figure 5: Optical layout of the AO-Module.

Instrument Overview
The Adaptive Optics Module
Optical layout

The AO-Module was developed in the ESO headquarter laboratory in Garching (Bonnet et al. 2003). It consists in an optical relay from the VLT Cassegrain focus to the SPIFFI entrance focal plane, which includes a deformable mirror conjugated to the telescope pupil. The curvatures of the 60 actuators are updated at 420 Hz to compensate for the aberrations produced by the turbulent atmosphere. The optical layout is shown in Fig. 5.

At the reflected focus, a pick-up lens mounted to a tri-axial linear stage collects the visible flux of the AO guide star, which is then imaged on the membrane mirror. The wavefront sensor box (mirrors M1 to M4) collimates the beam and re-images the pupil (conjugated to the deformable mirror) on the lenslet array. There, the flux is split among 60 sub-apertures and forwarded to a second array of lenslets, which image the sub-apertures on the cores of 60 optical fibers. The photons are then guided to 60 Avalanche Photo Diodes (APDs) located in a cabinet mounted to the instrument housing.

In closed loop, a speaker located at the exit of an acoustic cavity forces the membrane mirror to oscillate at 2.1kHz. As a result, the pupil plane moves back and forth along the optical axis allowing the lenslet array to intercept alternatively the intra- and extra-focal regions. An aberration in the wavefront would de-collimate the beam locally, causing the flux density to vary along the optical axis. As APDs are read out synchronously with the oscillations, the relative intensity difference between the intra- and extra-focal phases is proportional to the local wavefront curvature. This signal is used to generate the corrective command to the deformable mirror. The correction is updated at 420Hz, with a closed-loop bandwidth of 30 to 60Hz. The control gains are optimized for the actual atmospheric conditions and the guide-star brightness.

Additional opto-mechanical elements are already integrated in the AO-Module in view of the Laser Guide Star mode operations. They are not shown in the optical layout of Fig. 5.

**Performance demonstration on the sky**

The Infrared Test Camera (ITC) mounted to the AO-Module during the stand-alone commissioning run of June was used to demonstrate the performance of the AO-Module. The ITC provides direct imaging over a fairly large FOV (15×15 arcsec^2) with a sampling adapted to the diffraction-limited PSF in the near infrared (15 mas/pixel).

The typical AO-corrected PSF of a star features a diffraction-limited core superimposed on a larger halo generated by uncorrected high-order aberrations. The quality of the correction is evaluated with the Strehl ratio, computed as the fraction of the incoming energy which falls into the diffraction-limited core. In addition to the star brightness, the Strehl ratio is driven by the amplitude and the coherence time (τ_0) of the seeing: in poor seeing conditions, the PSF is blurred by the larger amplitude of the high-order aberrations, while the AO-Module reactivity becomes insufficient for fast seeing conditions.

The measured performance of the AO-

Figure 6: Strehl measurements obtained during AO-Module commissioning. Red squares show the specified Strehl performance. Black (resp. blue) dots are values obtained with $\tau_0 > 3$ ms (resp. $\tau_0 < 3$ ms)
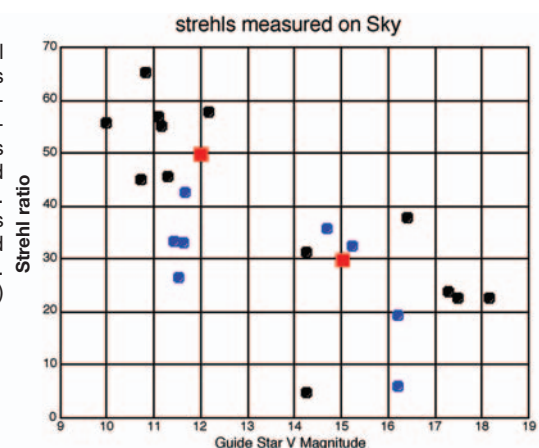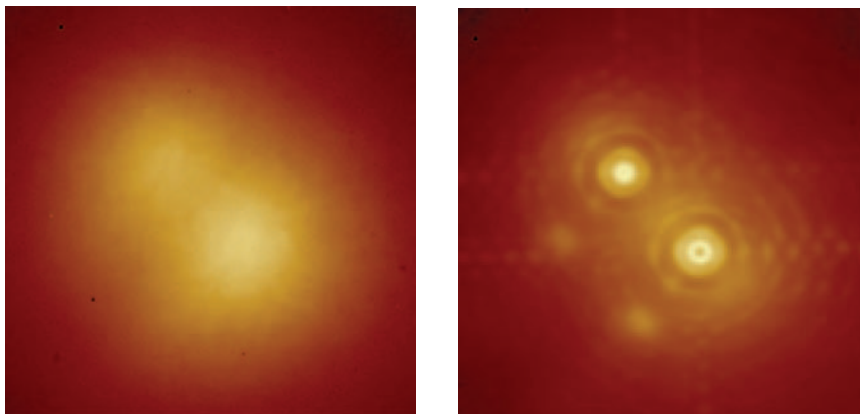
Figure 7: Observation of a binary system with a separation of 0.75″. To the left, open loop image acquired with a seeing of 0.6 arcsec. To the right, closed loop image obtained in the same conditions. The brighter component (lower right) served as a reference for the wavefront sensing. The additional "companions" at the lower left of the PSF cores are ghost images produced by a multiple reflection at the entrance window of the Infrared Test Camera.

Figure 8: Performance of AO-Module on faint guide star (visual magnitude 17.5). To the right, the seeing-limited K-band image (FWHM 0.38 arcsec). To the left, the AO-corrected image (FWHM 0.145 arcsec). The ability to perform AO corrections on very faint guide objects is essential for SINFONI observations of faint extragalactic objects.

Closed loop   Open loop

Ks-Band

FWHM=0.145"   FWHM=0.38"
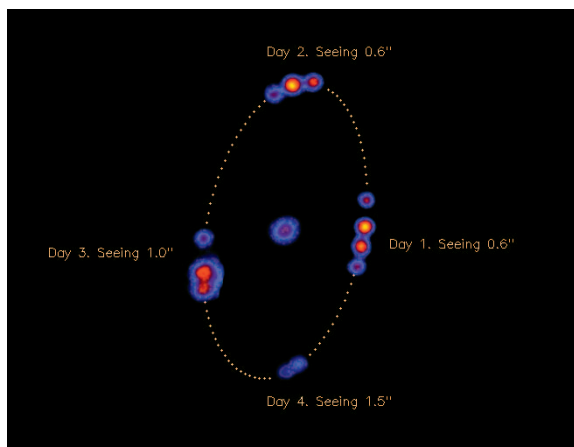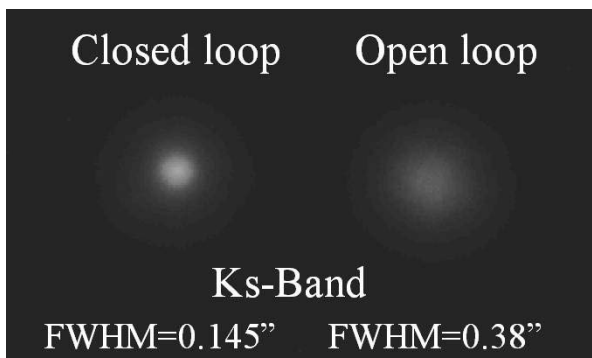
Figure 9: Image of asteroid Kalliope and its satellite Linus. The frames were acquired over four consecutive nights, surveying a complete orbital revolution of the system. The brightness of the central body (Kalliope) has been scaled down by a factor 15 to reduce the contrast with Linus. Changes in the size of the unresolved Linus image are due to variable seeing conditions from night to night.

appreciated from the number of visible Airy rings.

The ability to perform AO corrections on faint guide objects is essential for SINFONI in order to enable observations of faint extragalactic objects without nearby bright reference stars. This capability was demonstrated for good seeing conditions with a star of magnitude 17.5 (see Figure 8). The measured Full Width at Half Maximum (FWHM) of the corrected PSF in *K*-band was 0.145″ while the uncorrected FWHM was 0.38″.

Figure 9 shows the reconstructed 3.6-day orbit of Linus, a satellite of Kalliope. Kalliope is a 180km-diameter asteroid orbiting the sun from within the asteroid main belt, between the orbits of Mars and Jupiter, at nearly three times the Earth-Sun distance (three astronomical units). The binary system was observed in early June 2004 over four consecutive nights using the SINFONI AO module. Due to the geometry of the binary system at the time of the observations, the orbital plane of the satellite was seen at an angle of 60 degrees with respect to our line of sight. In fact, the satellite (~50km diameter) revolves around Kalliope on a 2000km-diameter circular orbit, with a direction of motion similar to the rotation spin of Kalliope (prograde rotation). The discovery of this asteroid satellite, named Linus after the son of Kalliope, the Greek muse of heroic poetry, was reported in September 2001 by a group of astronomers using the Canadian-France-Hawaii telescope in Hawaii (IAUC 7703). Additional observations of Kalliope have been obtained since 2001, which led to the determination of the main orbital characteristics of this binary system. Although Kalliope was previously thought to consist of metal-rich material, the discovery of Linus allowed scientists to derive a low ~2 g/cm^3 mean density for Kalliope. This number is inconsistent with a metal-rich object and Kalliope is now believed to be a rubble-pile stony asteroid. Its porous interior is due to a catastrophic collision with another smaller asteroid which occurred early in its history and gave birth to Linus. The VLT data obtained with the AO-Module of SINFONI will help refine our knowledge of the orbital characteristics and structural properties of this binary system.

Finally, the most impressive image so far was obtained during the August commissioning with SPIFFI: the Einstein Cross (Figure 10), a quadruple image of a single QSO amplified by the gravitational lensing induced by the foreground galaxy visible at the centre of the cross. This *H*-band reconstructed image was obtained with 20 minutes of integration time in the intermediate plate scale. The AO-Module was guiding on the brighter southern component, with a visual magnitude of 16. The total extension

Module is plotted vs. the guide-star magnitude in Fig. 6. Black dots are Strehl ratios obtained in conditions better than the median Paranal atmosphere, i.e. with a seeing < 0.65″ in the visible and a τ_0 > 3 ms, for which the AO-Module was specified (specifications are shown by the red squares). Strehl ratios obtained in degraded conditions are plotted in blue, for which the reduction in performance is larger than expected from the experience of the other MACAO systems. We believe that they were caused by a loss of bandwidth of the instrument induced by a variation of the membrane mirror gain between the laboratory and the telescope environmental conditions.

An illustration of the image quality achieved in good conditions with a bright reference star is given in Figure 7, which displays a pair of stars with similar magnitudes (~7.5) and a separation of 0.75″. The brightest component was used as the reference star, with an absorbing filter dimming the flux by 2.5 magnitudes to avoid saturating the detectors of the wavefront analyzer. The Strehl ratio cannot be estimated due to the saturated peak of the bright component, but the image quality can be qualitatively

Figure 10: Reconstructed H-band image of the Einstein cross obtained with SINFONI using the 100mas/pix mode (image size 3″x3″) under very good seeing conditions (0.45″). This image demonstrates the capability of the MACAO AO system to sharpen the images of faint astronomical objects (here the guide star is the brighter component and has V=16 mag). The Einstein cross was discovered in 1985 and is one of the best-known examples of gravitational lensing. A massive black hole at the centre of a nearby galaxy, located along the line of sight to a distant quasar, deforms the geometry of space in its immediate surroundings. As a result, the light from the quasar reaches us through different paths as if the quasar was observed through a kaleidoscope, creating multiple images of the same object. This special optics distorts and magnifies the light of background quasars, providing a means of probing the distribution of intervening matter in the cosmos.
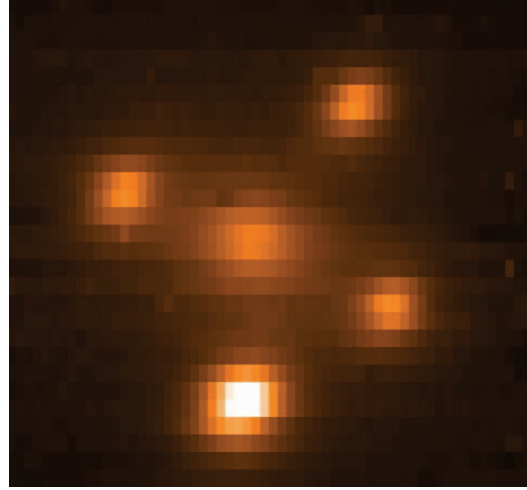
of the system is 1.8 arcsec, making it a very challenging target for the wavefront sensor due to its complex structure and low brightness. The seeing conditions were excellent during this integration (~0.5 arcsec with τ_0 ~ 4ms).

The near-infrared integral field spectrometer SPIFFI

SPIFFI was developed at the MPE (Eisenhauer et al. 2003) in collaboration with NOVA and ESO. It provides imaging spectroscopy of a contiguous, two-dimensional field of 64×32 spatial pixels in the wavelength range from $1.1 - 2.45$ µm at a resolving power of 2000 to 4000. As a result, the instrument delivers a simultaneous, three-dimensional data-cube with two spatial dimensions and one spectral dimension. Originally equipped with a 1024^2 pixel detector, SPIFFI was upgraded with a new camera unit built by NOVA and a HAWAII 2048^2 RG detector array from Rockwell in the two months between the SINFONI system tests in Garching and the commissioning in Paranal. The integral field unit of SPIFFI is a so-called mirror slicer (Tecza et al. 2002). This image slicer consists of two stacks of 32 plane mirrors, cutting the field of view into 32 narrow stripes and rearranging these slitlets to form a single long slit. Depending on the selected image scale, the FOV of the integral field unit ranges from $8'' \times 8''$ for seeing-limited observations to $0.8'' \times 0.8''$ for imaging spectroscopy at the diffraction limit of the VLT. The intermediate magnification with a $3.2'' \times 3.2''$ field of view provides a compromise between reduced spatial resolution and improved sensitivity, and is best-suited for AO-assisted observations of objects with low surface brightness. The slit width in the three image scales is 250, 100, and 25 mas, with equivalent pixel sizes of 125, 50, and 12.5 mas. SPIFFI is equipped with four directly ruled gratings optimized for covering the atmospheric *J, H, K,* and combined *H+K* bands in a single exposure. The spectral resolving power for the 250 mas slit width is about
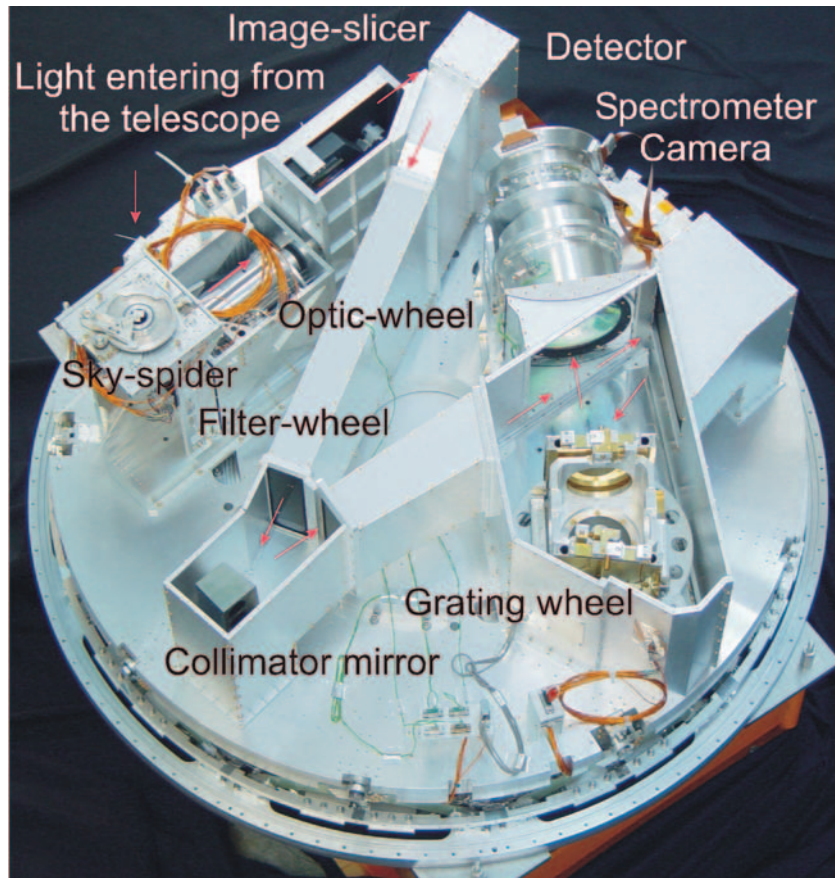
Figure 11: An inside view of SPIFFI: the cryostat cover and the reinforcing structure have been removed to provide a view of the opto-mechanical components of SPIFFI. The light enters from the top. The pre-optics with a filter-wheel and interchangeable lenses provides three different image scales. The image slicer rearranges the two-dimensional field into a pseudo-long slit, which is perpendicular to the base plate. Three diamond-turned mirrors collimate the light on the gratings. In total, four gratings are installed on the grating drive. A multiple-lens system then focuses the spectra on a Rockwell HAWAII array. In the meantime the spectrometer has been upgraded with an 2048^2 pixel detector and a new spectrometer camera. The diameter of the instrument vessel is 1.3 m.

2000 in *J*, 3000 in *H*, 4000 in *K*, and 2000 in *H+K*. When using the adaptive optics image scale, the spectral resolving power increases up to about 2400 in *J*, 5500 in *H*, 5900 in *K*, and 2700 in *H+K*, but spectral dithering is necessary to recover the full resolution from the undersampled spectra. The entire instrument is cooled with liquid nitrogen to a temperature of –195° C. Figure 11 shows an inside view of SPIFFI.

A quick-look image reconstruction allows the instantaneous display of the reconstructed image during acquisition and observing. SPIFFI is equipped with its own data-reduction software, which is presently implemented in the VLT data-reduction

Slit width	250 mas	100 mas	25 mas
J Band	18.0	18.5	17.0
H Band	17.5	18.5	17.3
K Band	16.9	18.0	17.2
H+K Band	17.7	18.9	18.2

Table 1: Limiting magnitudes for the observations of a point source. The sensitivities are calculated for a signal/noise of 10 per spectral channel and one hour integration on source (6 x 10 minutes, plus additional sky observations). We assume that 50%, 50%, and 25% of the flux is encircled within a diameter of 0.65″, 0.2″, and 0.1″ for seeing-limited observations with the 250 mas slitlets, and AO assisted observations with the 100 mas and 25 mas slitlets, respectively.

pipeline. This software package provides all tools for the calibration and reduction of SPIFFI data, including wavelength calibration and image reconstruction. The final data format is a three-dimensional data cube with 64×60 spatial pixels, and up to ~4500 spectral elements.

Table 1 lists the limiting magnitudes for the observation of a point source in the various instrument configurations.

FIRST SCIENCE FROM COMMISSIONING

In addition to performance characterization and optimization, the commissioning runs were used to explore the capabilities of the instrument via test observations on a selection of exciting astronomical targets.

DIFFRACTION-LIMITED INTEGRAL-FIELD SPECTROSCOPY OF THE GALACTIC CENTRE

Because of its proximity of only 8 kpc, the centre of the Milky Way is a unique laboratory for studying physical processes that are thought to occur generally in galactic nuclei. The central parsec of our Galaxy contains a dense star cluster with a remarkable number of luminous and young, massive stars, as well as several components of neutral, ionized and extremely hot gas. For two decades, evidence has been mounting that the Galactic Centre harbors a concentration of dark mass associated with the compact radio source SgrA* (diameter about 10 light minutes), located at the centre of that cluster. Measurements of stellar velocities and (partial) orbits with the ESO NTT (SHARP) and VLT (NACO) have established a compelling case that this dark mass concentration is a massive black hole of about $3.5 \cdot 10^6$ M$_\odot$ (Schödel et al. 2002). The Galactic Centre thus presently constitutes the best proof we have for the existence of massive black holes in galactic nuclei. High-resolution observations offer the unique opportunities

to stringently test the black-hole paradigm and study stars and gas in the immediate vicinity of a black hole, at a level of detail that will never be accessible in any other galactic nucleus. AO-assisted integral-field spectroscopy will play a unique role in studying this important region.

The Galactic Centre was observed during SINFONI commissioning on July 15, 2004, for about 2 hours in ~0.6″ seeing conditions. The AO-Module was locked on a 14.6 mag star located about 20″ to the north-east of SgrA* and the centre of the star cluster. We observed with the finest plate scale (0.0125″ × 0.025″ per pixel) and the H+K grating (resolving power ~2000). Figure 12 (left insets) shows the *K* cube collapsed into a quasi-continuum image whose FWHM resolution is 75 mas, i.e. very close to the diffraction limit of the VLT in the *K* band. The Strehl ratio was about 10% in *K* band but is wavelength dependent.

The SINFONI data provide for the first time a complete census of the near-IR spectra of most K ≤ 16 stars within about 20 light-days of the black hole. The right upper insets of Figure 1 show that a number of these "S-stars" exhibit HI Brγ (and HeI) absorption, characteristic of early type, O–B main sequence stars. In fact we find that at least 2/3 of all stars with K ≤ 16 in the central arcsecond have Brγ in absorption. This finding increases dramatically the 'paradox of youth' (Ghez et al. 2003), as to how these

massive and presumably young stars have managed to reside in the central few tens of light days around the black hole. A number of ideas have been put forward, including *in situ* formation in an extremely dense circumnuclear gas disc, in-spiraling of a massive young star cluster, perhaps aided by intermediate-mass black holes, scattering by stellar black holes, and collisional build-up of massive stars from lower-mass stars, but none is so far fully convincing. The orbital properties of the S-stars, now better constrained with the radial velocities obtained by SINFONI, promise to give important additional clues to the origin of the massive central star cluster.

Additional SINFONI observations on July 16 also provide new information on the spectral properties of massive blue supergiants further away from SgrA*. An AO-assisted observation of IRS13 E (lower right inset in Fig. 12), for the first time permitted spatially resolved spectroscopy of all three major components of this compact concentration of stars, which has been proposed to be the remnant core of an in-spiraling young star cluster. We find that all these three components have the characteristics of different types of Wolf-Rayet stars.

During the observations of July15 we had the good luck to catch a small flare of infrared radiation from SgrA* itself (lower left inset in Fig. 12). These infrared flares, seen for the first time in NACO observations last year (Genzel et al. 2003 b), probably sample in-falling hot gas in the immediate vicinity of the event horizon. By revealing the spectral properties of this flare the SINFONI data offer key new insights into the emission processes that cause infrared flares.

These few hours of data taken on the Galactic Centre during commissioning pro-

Figure 12: Diffraction-limited integral-field spectroscopy of the Galactic Centre with SINFONI. The background image shows a composite H,Ks,L'-band, three-colour image taken with the AO imager NACO, delineating the distribution of the different types of stars and the hot interstellar dust in the central parsec.
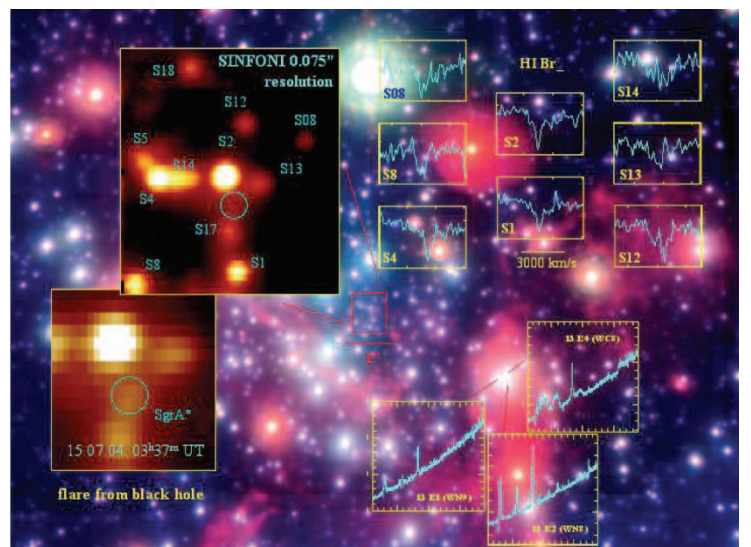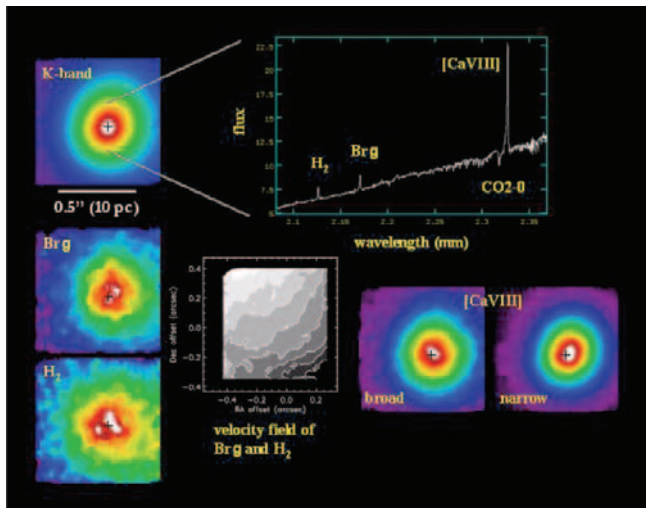
Figure 13: The Circinus galaxy - the nearest galaxy with an active centre (AGN) - was observed in the *K* band (2 μm) using the nucleus to guide the SINFONI AO-Module. The seeing was 0.5 arcsec and the width of each slitlet 0.025 arcsec; the total integration time on the galaxy was 40 min. At the top is a *K*-band image of the central arcsec of the galaxy (left insert) and a *K*-band spectrum of the nucleus (right). In the lower half are images (left) in the light of ionised hydrogen (Brγ) and molecular hydrogen (H₂) lines, together with their combined rotation curve (middle), as well as a CO 2-0 bandhead map, which traces cool stars in the nucleus, and images of broad and narrow components of the high-excitation [Ca VIII] spectral line (right). The false colours in the images represent regions of different surface brightness.

Figure 14: NGC 7469 was observed in *K* band (2 μm) using the nucleus as the wavefront reference for the adaptive optics and with slitlet widths of 0.025″. At the time of the observations the seeing was 1.1″. The total integration time on the galaxy is 1 hour 10 min. Upper left: image of the *K*-band continuum in the central arcsec of NGC 7469. Upper right: a spectrum extracted from the nucleus. Lower left: image of the molecular hydrogen line together with its rotation curve. Lower centre: image of the Brγ line. Lower right: image of the CO 2-0 absorption bandhead which traces cool stars.
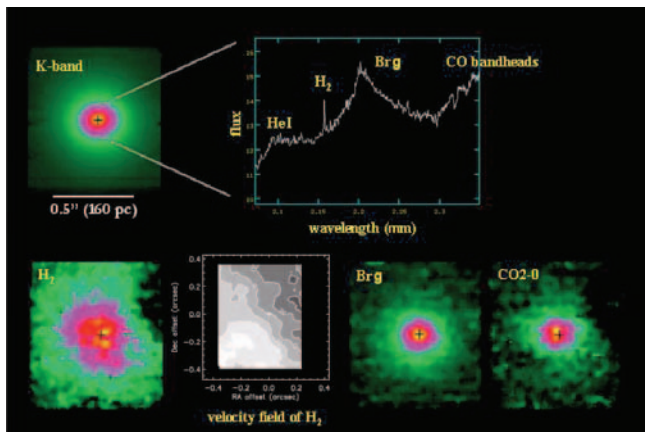
vide a small glimpse of the fantastic information that diffraction-limited spectroscopy will bring for Galactic Centre (and star cluster) research in the next few years. More will undoubtedly follow next year when the instrument becomes available for science exploitation.

A SHARP LOOK AT ACTIVE GALACTIC NUCLEI

The role of star formation in active galactic nuclei (AGN) has long been a contentious issue. Increasing evidence that starbursts do occur in the vicinity of at least some AGN has led to a change in thinking from the "starburst or black hole" debate of the last 10–20 years to a new framework in which the fundamental questions concern the physics linking the two phenomena. This is more than just an issue of driving gas in to small scales because AGN and star formation activity impact each other via feedback mechanisms. But the extent of this interaction can only be ascertained by addressing how common, how extended, how recent, and how energetically significant starbursts around AGN are. Commissioning observations of the Circinus galaxy and NGC 7469

demonstrate the potential of SINFONI to probe the environment around AGN on small scales, and to reveal in detail the distribution and dynamics of both the stellar and gaseous components.

The Circinus galaxy harbours a Seyfert 2 nucleus and, at a distance of only 4 Mpc, is one of the nearest such objects. Although the AGN itself is highly obscured, the compact K-band core also reveals the AGN indirectly, since it has a non-stellar origin: the distribution of the stellar continuum is revealed by the CO 2–0 absorption bandhead at 2.29 μm to have a much broader distribution. This more extended morphology is also reflected in the H₂ 1–0 S(1) 2.12μm line, as reported by Davies et al. (1998), and the Brγ 2.17 μm line. Because these lines are narrow and show ordered rotation, it is likely that they arise in a disc around the AGN. The position angle and speed of the rotation are consistent with those at larger radii, indicating that down to scales of a few parsecs there is no warp in the galactic plane. Circinus is known to exhibit a number of high-excitation coronal lines. Of these, the [CaVIII] line at 2.32 μm (the ionisation potential of which is 127 eV) is particularly

strong. An initial analysis of the line properties reveals an increase in the velocity and decrease in its dispersion from the nucleus to a region offset to the northwest. Our interpretation is that there are two components to this line: a broad component centred on the nucleus at the systemic velocity and probably associated with the Broad Line Region; and a narrow component, which is redshifted by an additional 140 km/s, offset in the direction of the prominent ionisation cone, and likely associated with it.

NGC 7469 is a prototypical Seyfert 1 galaxy at a distance 66 Mpc that is well known for its circumnuclear ring, as well as a significant contribution from star formation to the nuclear luminosity (e.g. Genzel et al. 1995). Recent adaptive optics long-slit spectra combined with a millimeter interferometric map of the cold gas (Davies et al. 2004) led to a dynamical model in which the gas forms two rings, at 2.5″ (800 pc) and 0.2″ (65 pc). In this interpretation, the nuclear star forming region, which contributes at least half of the mass within 30 pc of the nucleus, was confined within the inner ring. These results are confirmed by new data from SINFONI which reveal the full 2-

Figure 15: Image of the Galaxy pair BX 404/405 (redshift 2.03) in the light of the Hα recombination line (restframe wavelength 656 nm). One of the spectra (upper right) clearly reveals signs of a velocity shear while the other does not. Such shear may be a sign of rotation, a possible signature of a disc galaxy – or of a merger. The relatively small velocity offsets of the galaxies suggest that they are interacting and may perhaps merge to form a massive galaxy.
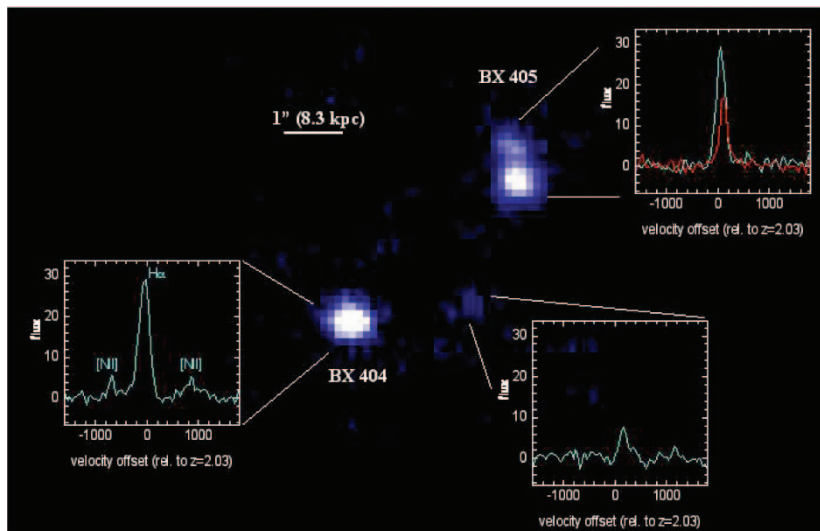
dimensional distributions of the H_2 1–0 S(1) line and the nuclear star forming region, through the CO 2–0 bandhead.

A Pair of Star-Forming Galaxies at z=2

It is becoming increasingly clear that most of the baryonic mass in galaxies was put in place between about 8 and 11 billion years ago (redshifts between 1 and 3). However, the real test of our understanding of galaxy formation and evolution is not just when the mass accumulated, but rather: How did it accumulate? Did mass assembly occur in the same way in different types of galaxies (i.e., spiral galaxies like the Milky Way and elliptical galaxies)? Was the mass accumulation rate mass-dependent so that more massive galaxies formed earlier in the history of the Universe? Why do some galaxies have large amounts of angular momentum, while others do not?

To address these questions, astrophysicists in Europe and the US have defined samples of galaxies that are at redshifts where most of the mass was likely put in place, namely around 2. For example, Steidel and collaborators have defined selection criteria based on three optical colours which efficiently select actively star-forming galaxies at redshifts between 1.5 and 2.5 (the so-called "BM and BX galaxies"; Steidel et al. 2004). Galaxies selected this way are forming stars at approximately 20–60 $M_\odot$/yr, appear to be substantially evolved with stellar masses of about 10^{11} $M_\odot$ and have approximately solar metallicity. All these properties suggest that they are highly evolved systems, even though their star-formation rates are substantial. In contrast, they tend to have complex UV morphologies and their dynamical properties are confusing – typical for galaxies that are rather unevolved. Interestingly, BM/BX galaxies with elongat-

ed, sometimes flattened morphologies like those usually associated with discs, appear to have smaller line widths than galaxies of more irregular shape. Erb et al. (2004) hypothesized that these galaxies are in the course of a merger, and not showing signs of systematic rotation which would be associated with a disc.

It is this last argument that led us to carry out observations with SINFONI of a pair of BX galaxies – BX 404/405 – during commissioning. Since the morphologies of BM/BX galaxies are complex and the most extended structures are not necessarily due to coherent rotation but to companion merging galaxies, it is difficult or even impossible to define the "kinematic major axis" (the angle along which the velocity change or gradient reaches its maximum). Exploiting SINFONI's integral field capability, one does not *a priori* have to choose a position angle, but simply puts the target in the field of view and then measures the source kinematics. If for example a system consists of a pair of merging galaxies, then there might even be two or more velocity components: Each galaxy could show a rotation curve of its own inclined by a different angle, and superimposed on the relative velocity along the line connecting the two galaxies. With such complicated objects, SINFONI is particularly powerful in determining the nature of the sources by obtaining the complete picture of the dynamics at once.

The galaxies BX 404 and 405 are especially interesting because this is an association of two star-forming galaxies at almost exactly the same redshift only about 3–4 arc seconds apart (about 30 kpc at this redshift). Thus we could cover both objects in a single pointing. What we found is fascinating: the relative velocity of BX 404 and 405 is only about 150 km/s. They are separated by about 30 kpc, while the emission-line object to the south and west of BX 404 and 405 has a

velocity of 150 km/s relative to BX405 and about 300 km/s relative to BX404. The two components of BX405 have velocities that differ by about 70 km/s, with a spatial separation of about 6 kpc. The velocity and size allow us to roughly estimate that BX405 has a dynamical mass of about 10^{10} $M_\odot$.

The overall similar velocities in this system suggest that this may be an interacting set of galaxies, which could merge to form a single more massive object. If BX 404 and 405 are part of a larger gravitationally bound structure, their relative velocities and projected distances suggest a total mass of about 10^{11} solar masses. In addition, the ratio of [NII]/Hα can be used to give a crude estimate of the gas-phase metal abundances. In BX 404, the [NII]/Hα line indicates a total metallicity similar to the Sun. We only have an upper limit for BX405, suggesting that its metallicity is less than that of BX 404 and the Sun.

Obviously, these results are only a first step: before any robust statement can be made, a statistically significant sample of such high-redshift galaxies will have to be observed. Nonetheless, these observations illustrate the great promise of SINFONI for obtaining a detailed picture of the properties of star-forming galaxies in the high-redshift Universe.

REFERENCES
H. Bonnet et al. 2003, SPIE 4839, 329
F. Eisenhauer et al. 2003, Proc. SPIE 4844, 1548
M. Tecza, et al. 2002, Proc. SPIE, 4842, 36
Davies et al. 1998, MNRAS, 293, 189
Davies et al. 2004, ApJ, 602, 148
Erb et al. 2004, accepted for publication ApJ (astro-ph/0404235)
Genzel et al. 1995, ApJ, 444, 129
Genzel, R. et al. 2003a, ApJ 594, 812
Genzel, R. et al. 2003b, Nature 425, 934
Ghez, A. et al. 2003, ApJ 586, L127
Schödel, R. et al. 2002, Nature 594, 812
Steidel, C. C. et al. 2004, ApJ, 604, 534